



Title	Effect of structural differences in collagen sponge scaffolds on tracheal epithelium regeneration( 本文 )
Author(s)	仲江川, 雄太
Citation	
Issue Date	2016-03-24
URL	<a href="http://ir.fmu.ac.jp/dspace/handle/123456789/536">http://ir.fmu.ac.jp/dspace/handle/123456789/536</a>
Rights	This is the accepted manuscript of the following article: Nakaegawa Y et al. Effect of Structural Differences in Collagen Sponge Scaffolds on Tracheal Epithelium Regeneration. Ann Otol Rhinol Laryngol. 2016 Feb;125(2):115-22. © The Author(s) 2015. doi: 10.1177/0003489415599991
DOI	
Text Version	ETD

Effect of structural differences in collagen sponge  
scaffolds on tracheal epithelium regeneration

コラーゲンスポンジスキヤフオールドの構造的差異が  
気管上皮再生に及ぼす影響

福島県立医科大学 医学部 耳鼻咽喉科学講座

仲江川 雄太

This is the peer reviewed version of the following article: Nakaegawa Y, Nakamura R, Tada Y,

Nomoto Y, Imaizumi M, Suzuki R, Nakamura T, Omori K.

Effect of structural differences in collagen sponge scaffolds on tracheal epithelium regeneration. Ann

Otol Rhinol Laryngol 2016 Feb;125(2):115-122. Copyright© 2015 (The Authors).

DOI:10.1177/0003489415599991.

Effect of structural differences in collagen sponge scaffolds on tracheal epithelium regeneration

Yuta Nakaegawa, MD <sup>1</sup>, Ryosuke Nakamura, PhD<sup>1</sup>, Yasuhiro Tada, MD, PhD <sup>1</sup>, Yukio Nomoto MD, PhD <sup>1</sup>, Mitsuyosi Imaizumi, MD, PhD <sup>1</sup>, Ryo Suzuki, MD <sup>1</sup>, Tatsuo Nakamura MD, PhD <sup>2</sup>, Koichi Omori, MD, PhD <sup>1</sup>

1, Department of Otolaryngology, Fukushima Medical University, Fukushima, Japan

2, Department of Bioartificial Organs, Institute for Frontier Medical Sciences, Kyoto University, Kyoto, Japan

Address: Hikarigaoka 1-Fukushimashi-Fukushima-Japan

TEL: +81-24-547-1321

FAX: +81-24-548-3011

E mail:nakaegaw@fmu.ac.jp

Keywords: collagen scaffold, Tissue regeneration, Tracheal Stenosis, laryngotracheal stenosis, Reconstruct

Presented at the meeting of the American Broncho-Esophagological Association, Boston Massachusetts. April 22-23, 2015.

Dr Nakaegawa received the Steven D. Gray Resident Award for 2015 from the Association.

## Abstract

### Objective

We developed an *in situ* regeneration-inducible artificial trachea composed of a porcine collagen sponge and polypropylene framework, and used it for tracheal reconstruction. In the present study, collagen sponges with different structures were prepared from various concentrations of collagen solutions and their effect on the regeneration of tracheal epithelium was examined.

### Methods

Collagen sponges were prepared from type I and III collagen solutions. The structures of the sponges were analyzed using scanning electron microscopy (SEM). Artificial tracheae, which were formed using the collagen sponges with different structures, were implanted into rabbits, and regeneration of the tracheal epithelium on the artificial tracheae was evaluated by SEM analysis and histological examination.

### Results

SEM analysis showed that collagen sponges prepared from 0.5% and 1.0% collagen solutions had a porous structure. However, the sponges prepared from a 1.5% collagen solution had a non-porous structure. After implantation of artificial tracheae prepared from 0.5% and 1.0% collagen solutions, their luminal surfaces were mostly covered with epithelium within 14 days. However, epithelial reorganization occurred later on artificial tracheae prepared from the 1.5% collagen solution.

### Conclusion

Collagen sponges with a porous structure are suitable for regeneration of the tracheal epithelium in our artificial trachea.

## Introduction

Tracheal resection and reconstruction are required in patients with malignant tumor or airway stenosis. Tracheal defects have conventionally been reconstructed by end-to-end anastomosis or autologous tissue implantation using skin or cartilage obtained from the nasal septum, auricle, or costal cartilage. However, recent studies have suggested that a tissue engineering technique is more effective for reconstruction of tracheal defects.<sup>1-7</sup>

We developed an *in situ* regeneration-inducible artificial trachea composed of a porcine collagen sponge and a polypropylene framework and have used it clinically for tracheal reconstruction.<sup>1-5</sup> These artificial tracheae made from collagen sponge have been applied successfully to patients with non-circumferential trachea resection.<sup>4,5</sup> However, slow regeneration on the luminal surface of the prosthesis remains a problem. The tracheal epithelium serves as a major protective barrier at the interface between the host and external environment, where tight junctions physically prevent the entry of pathogens and particles. Ciliated cells, the predominant cell type at the surface of the tracheal epithelium, contribute to mucociliary clearance. Therefore, delayed epithelial regeneration raises the risk of infection.

The important factors for tissue engineering are cells, regulation factors, and scaffolds.<sup>7</sup> To promote regeneration of the tracheal epithelium, our group has studied the effects of fibroblasts, adipose-derived stem cells, and basic-fibroblast growth factor in artificial grafts and have shown that they

shorten the time for epithelialization and cilia formation.<sup>8-14</sup> Collagen scaffolds are widely used in regenerative medicine because of their high biocompatibility but no studies have examined the most suitable structure of collagen scaffold for tracheal regeneration.

In this study, collagen sponges with different structures were prepared from various concentrations of collagen solutions and the effect of the collagen sponge structure on regeneration of the tracheal epithelium was examined.

## Materials and Methods

### *Collagen Sponges*

Collagen sponge was prepared as described previously with modifications.<sup>1-3</sup> Porcine atelocollagen (NH Foods Ltd., Ibaraki, Japan) consisted of type I collagen (70–80%) and type III collagen. Atelocollagen was dissolved in a hydrochloric acid solution (pH 3.0) to prepare 0.5%, 1.0%, and 1.5% atelocollagen solutions that were used to prepare the collagen sponges by freeze-drying for 96 h in a laboratory freeze-dryer (FDU-2200; TOKYO PIKAKIKAI Co., Ltd., Tokyo, Japan).

### *Artificial Trachea*

The procedure for the production of the artificial trachea has been described previously.<sup>2</sup> Briefly, the artificial trachea consisted of a Marlex mesh tube (pore size 260  $\mu\text{m}$ , polypropylene; Bard, Inc., Billerica, MA) reinforced with polypropylene rings and coated with collagen sponge.<sup>1,2</sup>

In the current study, a modified version of the artificial trachea was prepared for the rabbit model. The Marlex mesh tube was 35 mm long and had an outer diameter of 20 mm. The polypropylene rings, which had a diameter of 1 mm (G. KRAHMER GmbH, Buchholz, Germany), were attached to the cylinder by melting them at several points and further fixed using 7-0 polypropylene sutures (G. KRAHMER GmbH) along a 20 mm segment. The tube was covalently immobilized and then further physically coated with collagen sponge prepared from the 0.5%, 1.0%, and 1.5% atelocollagen solutions (referred to as 0.5-, 1.0-, and 1.5-scaffolds, respectively) (Fig. 1A, B).

### *Animal Experiments*

Animal care, housing, and surgical procedures were carried out in accordance with the Guidelines of the Animal Experiment Committee, Fukushima Medical University. The artificial trachea was implanted into 18 Japanese white rabbits (male, 11 weeks of age, 1.8–2.2 kg body weight; Japan SLC, Inc., Shizuoka, Japan). The rabbits were anesthetized by an intramuscular administration of a cocktail of medetomidine hydrochloride (0.2 mg/kg; Nippon Zenyaku Kogyo Co., Ltd., Fukushima, Japan), midazolam (1.0 mg/kg; Astellas Pharma, Inc., Tokyo, Japan), and butorphanol tartrate (0.2 mg/kg; Meiji Seika Pharma Co., Ltd., Tokyo, Japan). Tracheal defects of 5 mm in width and 10 mm in length were prepared in the anterior portion of the trachea (Fig. 1C). The artificial tracheae were laid on the tracheal defects and sutured in place (Fig. 1D).

At 14 or 28 days after implantation, the luminal surface of the implanted area was observed with a bronchoscope (VISERA ELITE; Olympus Co., Ltd., Tokyo, Japan). The rabbits were euthanized by an intramuscular injection of pentobarbital sodium (Kyoritsu Seiyaku Corporation, Tokyo, Japan), and the trachea along with the sternohyoid and sternothyroid muscles were resected *en bloc* for histological examination, immunofluorescence analysis, and scanning electron microscopy (SEM). One rabbit implanted with 1.5-scaffold could not be used for these examinations, because the rabbit died at 17 days post-implantation.

#### *Histological Examination*

The samples were fixed with 4% paraformaldehyde in phosphate buffered saline (pH 7.4) and embedded in paraffin. They were sliced into 4- $\mu$ m sections and subjected to hematoxylin and eosin (H&E) staining for light microscopic observation (BX-51; Olympus).

#### *Evaluation of Thickness of Regenerated Epithelium*

Mean value of epithelial thicknesses which were measured at the center and the points 100  $\mu$ m-away from the center of tracheal defect in H&E-stained section was determined as the thickness of regenerated epithelium. The thickness of regenerated epithelium was evaluated in 14 days-post-implantation samples obtained from each 3 rabbits in the 0.5-, 1.0- and 1.5-scaffold groups, and 28 days-post-implantation samples obtained from each three rabbits in the 0.5- and 1.0-scaffold groups and two rabbits in the 1.5-

scaffold group.

### *Antibodies*

The primary antibodies used for immunofluorescence analysis were mouse monoclonal antibodies against  $\beta$ 4-tubulin (Sigma Aldrich Co., LLC., St. Louis, MO), cytokeratin AE1/AE3 (Dako Japan, Tokyo, Japan), and occludin (Zymed Laboratories, Inc., South San Francisco, CA). An Alexa Fluor 594-conjugated goat anti-mouse secondary antibody was also used (Molecular Probes, Inc., Eugene, OR).

### *Immunofluorescence Analysis*

The sections were incubated with a blocking solution (Dainippon Pharmaceutical Corporation, Osaka, Japan) to saturate nonspecific sites. They were then exposed sequentially to the primary antibodies and secondary antibody for 60 min at 37 °C. Cell nuclei were counterstained with 4', 6-diamidino-2-phenylindole (Dojindo Laboratories, Kumamoto, Japan). Fluorescent images were obtained with a confocal laser scanning microscope A1R (Nikon Instech, Tokyo, Japan).

### *SEM*

The samples were fixed in a solution of 2% glutaraldehyde in 0.1 mol/L phosphate buffer (pH 7.2), and the luminal side of the trachea was exposed by cleaving the trachea in the direction of the long axis. The specimens were fixed with 1% osmium tetroxide (Wako Pure Chemical Industries, Ltd.,

Osaka, Japan) overnight, and they were then critical point-dried and coated with osmium. Observations of the samples using a scanning microscope (SU8220; Hitachi High Technologies Corporation, Tokyo, Japan) were performed at an accelerating voltage of 2 kV.

## Results

### *Structure of Collagen Sponges*

SEM analysis showed that collagen sponges prepared from the 0.5% and 1.0% atelocollagen solutions had a porous structure and their framework was constructed by the dynamically arranged collagen membranes (Fig. 2A, B). However, collagen sponges made from the 1.5% atelocollagen solution had a non-porous structure that was constructed with collagen membranes arranged in parallel. The inter-membrane spaces observed in all sponges were small (Fig. 2C).

### *Bronchoscopic Examination*

The scaffolds were implanted into rabbit tracheae, and bronchoscopic examination was performed for each group. At 14 days after implantation, epithelialization over a large area of the luminal implant surfaces in the 0.5- and 1.0-scaffold-implanted rabbits was observed, whereas a small amount of granulation tissue was seen on the surface of the implant in the 0.5-scaffold-implanted group (Fig. 3A, B). The implant surface in the 1.5-scaffold-implanted rabbits was occupied by a large amount of granulation tissue that caused airway stenosis (Fig. 3C).

At 28 days after implantation, the surface of the implants appeared to be entirely epithelized in the 0.5- and 1.0-scaffold groups (Fig. 3D, E) but a small amount of granulation tissue was still observed on the luminal surface of the implants in the 1.5-scaffold group (Fig. 3F).

### *Histological Examination*

At 14 days after implantation, stratified squamous epithelium was observed on the luminal surface of the implants in the 0.5-scaffold group (Fig. 4A). The cells on the surface of the implants were positively stained with anti-cytokeratin AE1/AE3 that reacts with most cytoke­ratin family molecules, thus confirming epithelialization. Only a few epithelial cells were positive for  $\beta$ 4-tubulin, a marker for ciliated cells, but cilia were barely formed in these cells. Occludin was detected in the apical region of newly-formed epithelium, indicating that tight junctions were organized in the epithelium. Stratified squamous epithelium was also observed in the 1.0-scaffold group (Fig. 4B), but cilia were formed on several epithelial cells. Occludin was detected in the apical region of the epithelium in the 1.0-scaffold group. Conversely, no epithelium was observed on the implant surface of the 1.5-scaffold group (Fig. 4C). A few cytoke­ratin-positive cells were detected in the granulation tissue, but not on the luminal surface. Furthermore, ciliated cells were not detected in this group.

At 28 days after implantation, a pseudostratified epithelium with columnar ciliated cells was observed on the implant surfaces in the 0.5- and 1.0-scaffold groups (Fig. 4D, E). The luminal surface of the trachea was mostly

covered with ciliated cells in these groups, and occludin was detected in the apical region of the epithelial cells. In the 1.5-scaffold group, epithelial tissue covered the luminal surface of the implants, and tight junctions were organized in the epithelial tissue (Fig. 4F). However, the epithelium formed in this group was squamous and had a small number of ciliated cells.

#### *Thickness of Regenerated Epithelium*

At 14 days after implantation, the thicknesses of regenerated epithelia in the 0.5- and 1.0-scaffold groups were in the ranges of 12.5–17.9 and 8.1–19.3  $\mu\text{m}$ , respectively (Fig. 4G). However, regenerated epithelia were 0  $\mu\text{m}$  thick in three of the three rabbits implanted with 1.5-scaffold. At 28 days after implantation, the thicknesses of regenerated epithelia in the 0.5-, 1.0- and 1.5-scaffold groups were in the ranges of 15.6–21.8, 19.3–29.3 and 15.0–20.6  $\mu\text{m}$  (Fig. 4H).

#### *SEM*

SEM analysis further confirmed epithelialization in the 0.5- and 1.0-scaffold groups and cilia formation in the 1.0-scaffold group at 14 days after implantation (Fig. 5A, B). Epithelialization was poor in the 1.5-scaffold group, and fibrous structures were exposed on the surface of the implants (Fig. 5C).

At 28 days after implantation, the luminal surface was predominantly covered by mature cilia in the 0.5- and 1.0-scaffold groups. Although epithelialization was observed in the 1.5-scaffold group, ciliated cells were

sparse, and the cilia that formed in these cells were immature.

## Discussion

Resection of part of the trachea in association with a malignant tumor or inflammatory lesion can result in functional disorders of speech, deglutition, and respiration. We developed an *in situ* regeneration-inducible artificial trachea made from collagen sponge and polypropylene which has been applied successfully to patients with non-circumferential trachea resection.<sup>4,5</sup>

In this study, the effect of collagen sponge structure on regeneration of the tracheal epithelium was examined. The collagen sponges prepared from 0.5% and 1.0% collagen solutions was porous. When these sponges were implanted in a partial defect of rabbit trachea, the luminal surface of the implants was mostly covered with newly formed epithelial tissue within 14 days. In contrast, collagen sponges prepared from the 1.5% collagen solution had a non-porous structure and epithelium formation on the non-porous sponges took longer than 14 days. Moreover, when thickness of regenerated epithelium was used as an index of epithelialization, epithelialization levels in the groups implanted with porous collagen sponge (0.5- and 1.0-scaffold groups) were higher as compared with non-porous collagen sponge-implanted group (1.5-scaffold group). These results suggest that a concentration of collagen greater than 1.5% is too dense for preparation of a porous structure, and that a porous structure is better for regenerating the tracheal epithelium. For tissue engineering, scaffolds should balance mechanical function and

permeability of biofactors (e.g., cells and cytokines)<sup>15</sup>. Many *in vitro* and *in vivo* studies have shown that a porous structure is necessary for cell invasion and growth. For example, Yamane et al.<sup>16</sup> fabricated porous scaffolds with chitosan-hyaluronic acid hybrid polymer fibers and concluded that a scaffold with a pore size of 400  $\mu\text{m}$  is suited to cartilage tissue engineering. Seung Hyun Ahn et al.<sup>17</sup> reported that a highly porous 3D collagen scaffold is suitable for the *in vitro* organization of a skin equivalent. Our results suggest that a porous structure is suitable for tracheal regeneration, similar to the regeneration of many other organs. In our implantation model, implanted collagen sponges initially played a role for substituent of tracheal mesenchyme. Mesenchymal cells invade into the defect before epithelial cell re-coverage during the process of tracheal regeneration similar to wound healing, and reorganize mesenchymal tissue to provide the basis for epithelial cells<sup>18,19</sup>. Additionally, mesenchymal cells are known to secrete various growth factors and cytokines, such as FGFs and HGF, which stimulate epithelial cell migration, growth and differentiation, during wound repair<sup>20,21</sup>. Indeed, our group has previously shown that stratification, basement membrane reconstruction, apicobasal polarization and cilia formation of cultured tracheal epithelial cells were promoted by co-culture with fibroblasts<sup>10</sup>. Moreover, following study has indicated that mesenchymal cells stimulate growth and the differentiation of tracheal epithelial cells during tracheal regeneration in a rat tracheal defect model<sup>22</sup>. Thus, mesenchymal cell invasion is an essential event for epithelial regeneration. Because a porous structure permits mesenchymal cell invasion into the sponge<sup>16,17</sup>, it

may be possible that collagen sponge with porous structure might provide a substitutional mesenchyme which is suitable for mesenchymal cell invasion, and indirectly promote epithelialization. The cell invasion is easier with porous structure than with non-porous structure.

Epithelial regeneration is achieved through epithelial cell growth and differentiation. Epithelial cell growth takes place primarily to cover defective regions, but is pre-requisite for epithelial cell differentiation and reorganization of functional epithelium<sup>18,23</sup>. Following to the epithelial cell stratification, epithelial cells differentiate into ciliated cells<sup>24</sup>, which are predominant in the luminal surface of normal trachea, and important in airway host defensive function as a vital component of mucociliary apparatus. Our data indicated that epithelial thickness was similar level in the 0.5- and 1.0-scaffold groups at 14 days post-implantation, but ciliated cells were more abundant in 1.0-scaffold group. Taken together, it is suggested that epithelial cells covered the defect more rapidly in 1.0-scaffold group than in 0.5-scaffold group. Although structural difference between the sponges prepared from 0.5 and 1.0% collagen could not be found by SEM, there might be a subtle structural difference between them. It is known that the structure of collagen sponge scaffold varies according to collagen concentrations and making processes such as the temperature or the time of freeze-drying<sup>25,26</sup>. Because the making process of the collagen sponges in this study is identical, structural difference in the collagen sponges depends on collagen concentrations. It is well-accepted that the pore size in collagen can dramatically affect cell behavior encouraging cell migration and

penetration into the scaffold <sup>27,28</sup>.

End-to-end anastomosis is a conventional method to reconstruct circumferential tracheal defects, which is caused by resecting cancer or stenotic region. Since this method is chosen for the defects of up to 6 cm in adults, one of goal for artificial trachea implantation is to regenerate over 6-cm long circumferential defects<sup>29</sup>. Epithelial regeneration in circumferential defects would be somewhat different from that in patch defect. It requires longer period. Force acting on artificial trachea would be different between circumferential and patch defect. In this study, just patch defect model was used to investigate the effects of collagen sponges on tracheal epithelialization. Further examination using circumferential defect model remains to be performed.

## Conclusion

The effect of the collagen sponge structure on regeneration of the tracheal epithelium was examined in our artificial trachea composed of a porcine collagen sponge and a polypropylene framework. Different collagen concentrations result in distinct structures of collagen sponge scaffolds. Collagen sponges with a porous structure appear to be suitable for regeneration of the tracheal epithelium.

## Acknowledgements

We thank Ms. Etsuko Sato for her technical assistance.

This work was financially supported by Fukushima Medical University.

## References

1. Okumura N, Nakamura T, Shimizu Y, et al. Experimental study on a new tracheal prosthesis made from collagen-conjugated mesh. *J Thorac Cardiovasc Surg.* 1994;108: 337-45.
2. Teramachi M, Nakamura T, Shimizu Y, et al. Porous-type tracheal prosthesis sealed with collagen sponge. *Ann Thorac Surg.* 1997;64: 965-69.
3. Nakamura T, Teramachi T, Sekine T, et al. Artificial trachea and long term follow-up in carinal reconstruction in dogs. *Int J Artif Organs.* 2000; 23: 718-24.
4. Omori K, Nakamura T, Knanemaru S. et al. Regenerative medicine of the trachea: the first human case. *Ann Otol Rhinol Laryngol.* 2005; 114: 429-33.
5. Omori K, Tada Y, Suzuki T, et al. Clinical application of in situ tissue engineering using a scaffolding technique for reconstruction of the larynx and trachea. *Ann Othol Rhino Laryngol.* 2008; 117: 673-78.
6. Macchiarini P, JUngebluth P, Go T, et al. Clinical transplantation of a tissue-engineered airway. *Lancet* 2008; 372: 2023-30.
7. Langer R, Vacanti JP. Tissue engineering. *Science.* 1993; 260:920-926.
8. Nomoto Y, Suzuki T, Tada Y, et al. Tissue engineering for regeneration of the tracheal epithelium. *Ann Otol Rhinol Laryngol.* 2006; 115:501-06.

9. Nomoto Y, Kobayashi K, Omori K, et al. Effect of fibroblasts on epithelial regeneration on the surface of a bioengineered trachea. *Ann Otol Rhinol Laryngol*. 2008; 117:59-64.
10. Kobayashi K, Nomoto Y, Suzuki T, et al. Effect of fibroblasts on tracheal epithelial regeneration *in vitro*. *Tissue Eng*. 2006; 1: 2619-28.
11. Okano W, Nomoto Y, Omori K, et al. Bioengineered trachea with fibroblasts in a rabbit model. *Ann Otol Rhinol Laryngol*. 2009; 118: 796-804.
12. Kobayashi K, Suzuki T, Omori K, et al. A tissue-engineered trachea derived from a framed collagen scaffold, gingival fibroblasts and adipose-derived stem cells. *Biomaterials*. 2010; 31: 4855-63.
13. Suzuki T, Kobayashi K, Omori K, et al. Regeneration of the trachea using a bioengineered scaffolds with adipose-derived stem cells. *Ann Otol Rhinol Laryngol*. 2008; 117: 453-63.
14. Tani A, Tada Y, Takezawa T, et al. Regeneration of tracheal epithelium using a collagen vitrigel-sponge scaffold containing basic fibroblast growth factor. *Ann Oto Rhinol Laryngol*. 2012; 123:1469-73.
15. A. Scott J. Hollister. Porous scaffold design for tissue engineering. *Nat Mater*. 2005; 4: 518-24.
16. Yamane S, Iwasaki N, Kasahara Y, et al. Effect of pore size on *in vitro* cartilage formation using chitosan-based hyaluronic acid hybrid polymer fibers. *J Bio Mate Res PartA*. 2006; 586-93.
17. SeungHyun Ahn, Hyeon Yoon, GeunHyung Kim, et al. Designed three-dimensional collagen scaffolds for skin tissue regeneration. *Tissue Eng*.

2010; 16: 813-20.

18. Laplante A.F, Germain L, Auger F.A. Mechanisms of wound reepithelialization: hints from a tissue-engineered reconstructed skin to long-standing questions. *FASEB J.* 2001; 15:2377-89.
19. David J. Geer, Daniel D. Swartz, Stelios T. Andreadis. In vivo model of wound healing based on transplanted tissue-engineered skin. *Tissue Eng.* 2004; 10: 1006-17.
20. Nishimura T. Soda S. Effects of hepatocyte growth factor, transforming growth factor-beta1 and epidermal growth factor on bovine corneal epithelial cells under epithelial-keratocyte interaction in reconstruction culture. *Exp.Eye Res.* 1998; 66: 105-116.
21. Steven W. Lisha, C. Rajiv, R Mohan. Expression of HGF, KGF, EGF and receptor messenger RNAs following corneal epithelial wounding. *Exp. Eye Res.* 1999; 68: 377-97.
22. Kobayashi, K., Suzuki, T., Nomoto, Y.et al. A tissue-engineered trachea derived from a framed collagen scaffold, gingival fibroblasts and adipose-derived stem cells .*Biomaterials.* 2010; 31:4855-63.
23. Geer D.J, Swartz D.D, Andreadis S.T. In vivo model of wound healing based on transplanted tissue-engineered skin. *Tissue Eng.*2004: 10:1006-1017.
24. Mercer R.R, Russell M.L, Roggli V.L. Cell number and distribution in human and rat airways. *Am J Respir Cell Mol Biol.* 1994; 10:613-24.
25. Steven T. Boyce, Deborah J. Christianson, John F. Hansbrough. Structure of a collagen-GAG dermal skin substitute optimized for

- cultured human epidermal keratinocytes. *J.Biomed.Mater.Res.* 1988;22:939-57.
26. Marta M, Alessandro S, Ioannis V.et al. Collagen-based matrices with axially oriented pores. *J.Biomed Mater Research Part A.* 2008; 85A: 757-67.
  27. Hubbel JA. Biomaterials in tissue engineering. *Bio/Technology(Nature Publishing Company).*1995; 13: 565-76.
  28. Berthod.F, Saintigny, F.Chretien, D Hayek. et al. Optimization of thickness, Pore size and Mechanical properties of a Biomaterial designed for deep burn coverage. *Clinical Materials* 1994; 15: 259-65.
  29. Teramachi M, Nakamura T, Shimizu Y, et al. Porous-type tracheal prosthesis sealed with collagen sponge. *Ann Thorac Surg.* 1997; 64: 965-69.

## Figure Legends

Figure 1. Implantation of an artificial trachea into a rabbit.

A) Tracheal prosthesis. B) Tracheal prosthesis coated with porcine collagen sponge. C) Tracheal defect, approximately 5 mm in width and 10 mm in length. D) Defects were covered with three types of scaffold.

Figure 2. Scanning electron microscopy of collagen sponges.

A) 0.5% collagen sponge. B) 1.0% collagen sponge. C) 1.5% collagen sponge.  
Bars: 100  $\mu\text{m}$ .

Figure 3. Bronchoscopic examination at 14 and 28 days post-implantation.

Area of regeneration is shown between arrowheads.

A, B, C) Images from the 0.5-, 1.0-, and 1.5-scaffold groups at day 14, respectively. D, E, F) Images from the 0.5-, 1.0-, and 1.5-scaffold groups at day 28, respectively.

Figure 4. Histological analysis of the regenerated area.

A, B, C) 0.5-, 1.0-, and 1.5-scaffold groups at day 14, respectively. D, E, F) 0.5-, 1.0-, and 1.5-scaffold groups at day 28, respectively. The results of H & E staining and immunostaining for cytokeratin,  $\beta$ 4-tubulin, and occludin are

shown. In the images of the immunostained sections, red and blue indicate immunostaining and cell nuclei, respectively. In the images of immunostaining for cytokeratin, bright-field images are merged. Bars, 100  $\mu\text{m}$  and 10  $\mu\text{m}$  in images of H&E and immunostaining, respectively. G, H) Data plot of the thicknesses of regenerated epithelia at 14 and 28 days.

Figure 5. Scanning electron microscopy images of tracheal epithelium. A, B, C) 0.5-, 1.0-, and 1.5-scaffold groups at day 14, respectively. D, E, F) 0.5-, 1.0-, and 1.5-scaffold groups at day 28, respectively. Bars: 20  $\mu\text{m}$ .

# Artificial trachea

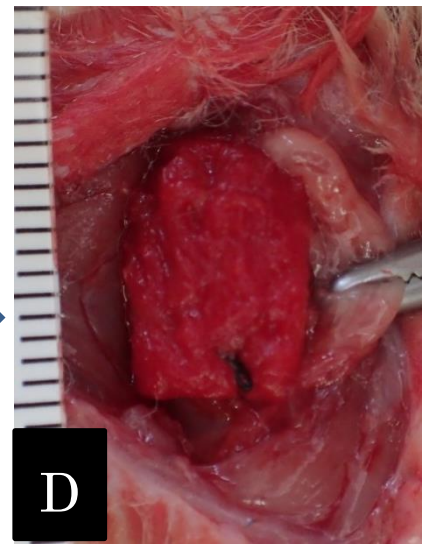
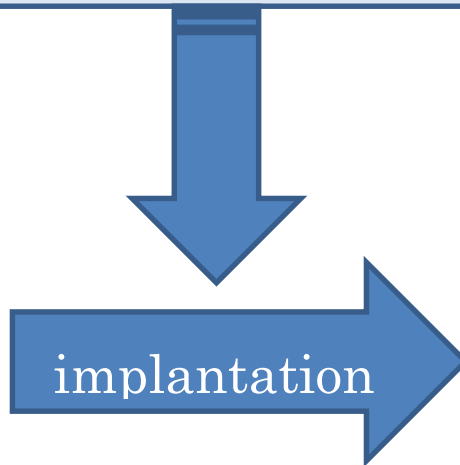
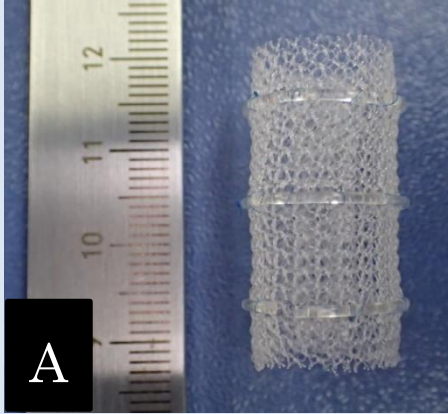


Figure 1

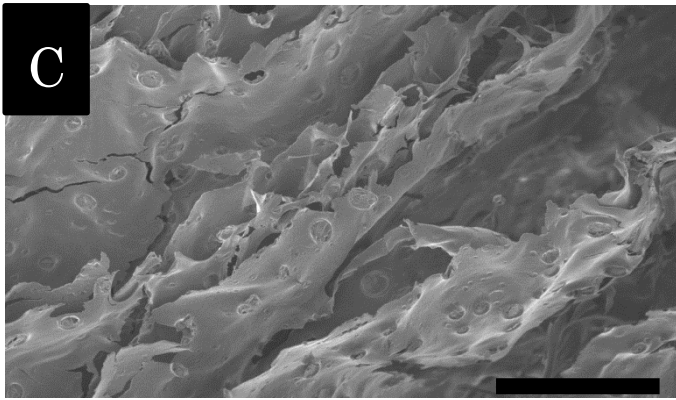
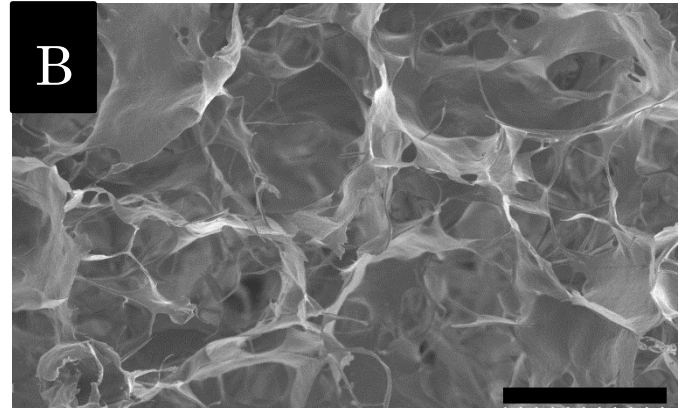
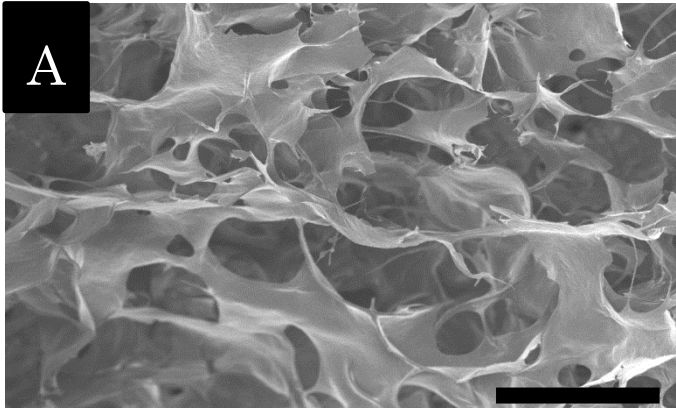


Figure 2

Figure 3

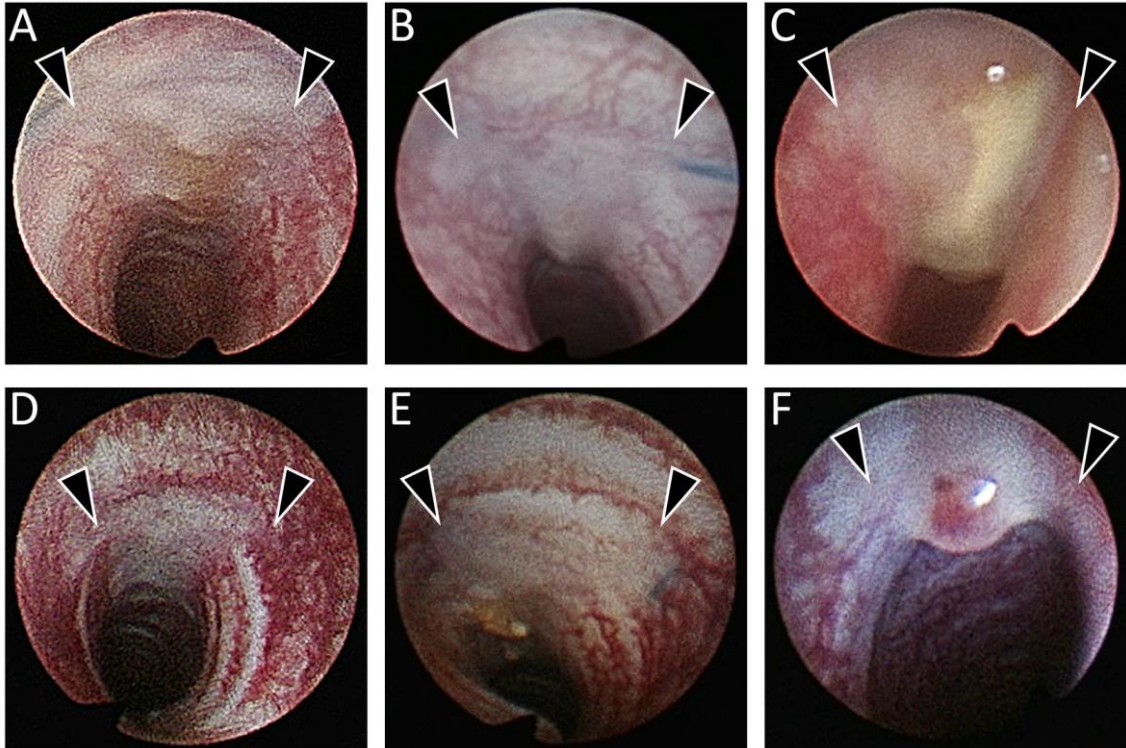


Figure 4

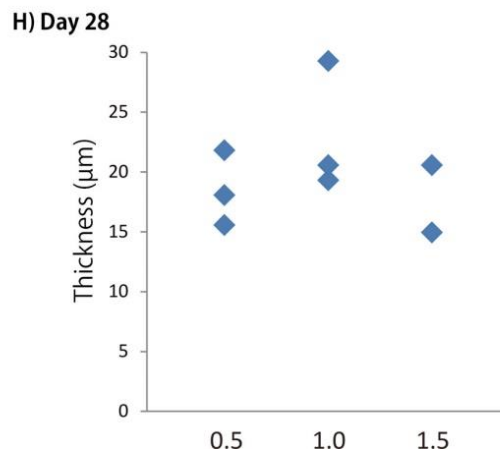
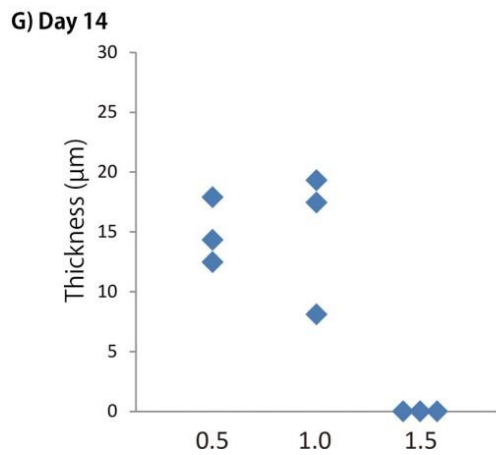
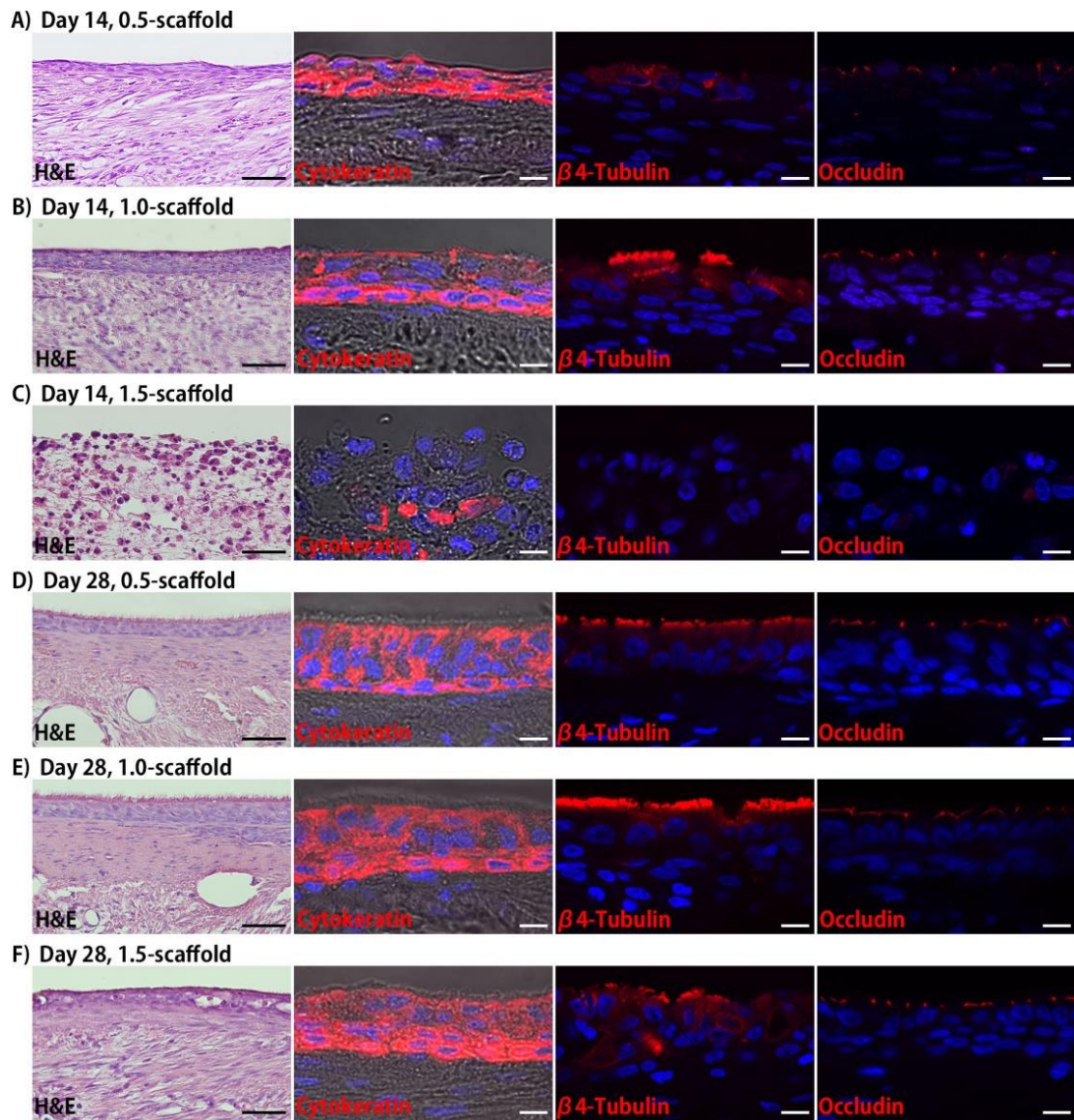


Figure 5

